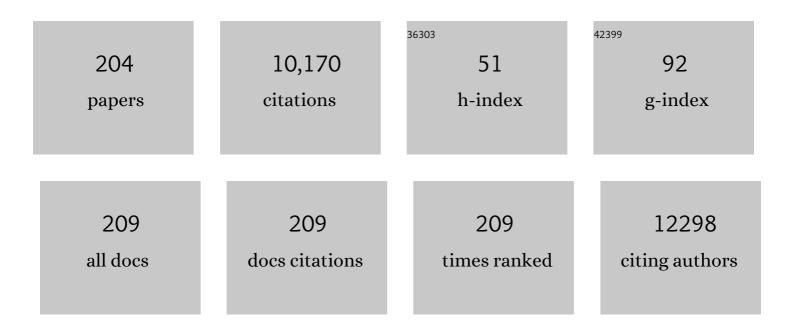


## List of Publications by Year in descending order

Source: https://exaly.com/author-pdf/4212500/publications.pdf Version: 2024-02-01



1.1.0

#	Article	IF	CITATIONS
1	Review on solid electrolytes for all-solid-state lithium-ion batteries. Journal of Power Sources, 2018, 389, 198-213.	7.8	964
2	The electrocapacitive properties of graphene oxide reduced by urea. Energy and Environmental Science, 2012, 5, 6391-6399.	30.8	460
3	Nanoflaky MnO2/carbon nanotube nanocomposites as anode materials for lithium-ion batteries. Journal of Materials Chemistry, 2010, 20, 6896.	6.7	413
4	Synthesis of porous hollow Fe3O4 beads and their applications in lithium ion batteries. Journal of Materials Chemistry, 2012, 22, 5006.	6.7	224
5	Harmonizing Energy and Power Density toward 2.7 V Asymmetric Aqueous Supercapacitor. Advanced Energy Materials, 2018, 8, 1702630.	19.5	201
6	Anisotropic Co3O4 porous nanocapsules toward high-capacity Li-ion batteries. Journal of Materials Chemistry, 2010, 20, 1506.	6.7	193
7	Development of solid-state electrolytes for sodium-ion battery–A short review. Nano Materials Science, 2019, 1, 91-100.	8.8	188
8	A high-energy-density supercapacitor with graphene–CMK-5 as the electrode and ionic liquid as the electrolyte. Journal of Materials Chemistry A, 2013, 1, 2313.	10.3	186
9	High–energy density nonaqueous all redox flow lithium battery enabled with a polymeric membrane. Science Advances, 2015, 1, e1500886.	10.3	186
10	Enhanced Multiferroic Properties and Valence Effect of Ru-Doped BiFeO <sub>3</sub> Thin Films. Journal of Physical Chemistry C, 2010, 114, 6994-6998.	3.1	181
11	Polyvinylpyrrolidone-Induced Uniform Surface-Conductive Polymer Coating Endows Ni-Rich LiNi <sub>0.8</sub> Co <sub>0.1</sub> Mn <sub>0.1</sub> O <sub>2</sub> with Enhanced Cyclability for Lithium-Ion Batteries. ACS Applied Materials & Interfaces, 2019, 11, 12594-12604.	8.0	173
12	Fe <sub>3</sub> O <sub>4</sub> Nanoparticles Embedded in Uniform Mesoporous Carbon Spheres for Superior Highâ€Rate Battery Applications. Advanced Functional Materials, 2014, 24, 319-326.	14.9	165
13	Graphene-based surface modification on layered Li-rich cathode for high-performance Li-ion batteries. Journal of Materials Chemistry A, 2013, 1, 9954.	10.3	163
14	A Na+ Superionic Conductor for Room-Temperature Sodium Batteries. Scientific Reports, 2016, 6, 32330.	3.3	160
15	Recent Progress in the Applications of Vanadiumâ€Based Oxides on Energy Storage: from Lowâ€Đimensional Nanomaterials Synthesis to 3D Micro/Nanoâ€Structures and Freeâ€Standing Electrodes Fabrication. Advanced Energy Materials, 2017, 7, 1700547.	19.5	151
16	Ru <sub>0.01</sub> Ti <sub>0.99</sub> Nb <sub>2</sub> O <sub>7</sub> as an intercalation-type anode material with a large capacity and high rate performance for lithium-ion batteries. Journal of Materials Chemistry A, 2015, 3, 8627-8635.	10.3	131
17	Composite Solid Polymer Electrolyte with Garnet Nanosheets in Poly(ethylene oxide). ACS Sustainable Chemistry and Engineering, 2019, 7, 7163-7170.	6.7	131
18	Lithium storage capability of lithium ion conductor Li1.5Al0.5Ge1.5(PO4)3. Journal of Alloys and Compounds, 2010, 501, 255-258.	5.5	127

#	Article	IF	CITATIONS
19	Electrochemical Properties of Nonstoichiometric LiNi[sub 0.5]Mn[sub 1.5]O[sub 4â^îî] Thin-Film Electrodes Prepared by Pulsed Laser Deposition. Journal of the Electrochemical Society, 2007, 154, A737.	2.9	117
20	Composite NASICON (Na <sub>3</sub> Zr <sub>2</sub> Si <sub>2</sub> PO <sub>12</sub> ) Solid-State Electrolyte with Enhanced Na <sup>+</sup> Ionic Conductivity: Effect of Liquid Phase Sintering. ACS Applied Materials & Interfaces, 2019, 11, 40125-40133.	8.0	115
21	One-step synthesis of hollow porous Fe3O4 beads–reduced graphene oxide composites with superior battery performance. Journal of Materials Chemistry, 2012, 22, 17656.	6.7	104
22	Advances in lead-free pyroelectric materials: a comprehensive review. Journal of Materials Chemistry C, 2020, 8, 1494-1516.	5.5	101
23	Advanced electrochemical performance of Li4Ti5O12-based materials for lithium-ion battery: Synergistic effect of doping and compositing. Journal of Power Sources, 2014, 248, 1034-1041.	7.8	99
24	Li <sub>4</sub> Ti <sub>5</sub> O <sub>12</sub> -based anode materials with low working potentials, high rate capabilities and high cyclability for high-power lithium-ion batteries: a synergistic effect of doping, incorporating a conductive phase and reducing the particle size. Journal of Materials Chemistry A, 2014, 2, 9982-9993.	10.3	97
25	A study of the superior electrochemical performance of 3 nm SnO <sub>2</sub> nanoparticles supported by graphene. Journal of Materials Chemistry A, 2014, 2, 5688-5695.	10.3	96
26	The Solvent Induced Interâ€Dimensional Phase Transformations of Cobalt Zeoliticâ€Imidazolate Frameworks. Chemistry - A European Journal, 2017, 23, 10638-10643.	3.3	95
27	A hybrid polymer/oxide/ionic-liquid solid electrolyte for Na-metal batteries. Journal of Materials Chemistry A, 2017, 5, 6424-6431.	10.3	93
28	Facile synthesis of chain-like LiCoO2 nanowire arrays as three-dimensional cathode for microbatteries. NPG Asia Materials, 2014, 6, e126-e126.	7.9	90
29	Synthesis of SnO <sub>2</sub> /MoS <sub>2</sub> composites with different component ratios and their applications as lithium ion battery anodes. Journal of Materials Chemistry A, 2014, 2, 17857-17866.	10.3	90
30	Effect of Li3PO4 coating of layered lithium-rich oxide on electrochemical performance. Journal of Power Sources, 2017, 341, 147-155.	7.8	90
31	On the fragmentation of active material secondary particles in lithium ion battery cathodes induced by charge cycling. Extreme Mechanics Letters, 2016, 9, 449-458.	4.1	86
32	Ultrathin VO <sub>2</sub> nanosheets self-assembled into 3D micro/nano-structured hierarchical porous sponge-like micro-bundles for long-life and high-rate Li-ion batteries. Journal of Materials Chemistry A, 2017, 5, 8307-8316.	10.3	86
33	Failure Mechanism and Interface Engineering for NASICON-Structured All-Solid-State Lithium Metal Batteries. ACS Applied Materials & Interfaces, 2019, 11, 20895-20904.	8.0	83
34	Polyanion Sodium Vanadium Phosphate for Next Generation of Sodiumâ€Ion Batteries—A Review. Advanced Functional Materials, 2020, 30, 2001289.	14.9	83
35	Hydrothermal synthesis of nanostructured graphene/polyaniline composites as high-capacitance electrode materials for supercapacitors. Scientific Reports, 2017, 7, 44562.	3.3	76
36	Nano-structural changes in Li-ion battery cathodes during cycling revealed by FIB-SEM serial sectioning tomography. Journal of Materials Chemistry A, 2015, 3, 18171-18179.	10.3	74

#	Article	IF	CITATIONS
37	X-ray diffraction and photoelectron spectroscopic studies of (001)-oriented Pb(Zr0.52Ti0.48)O3 thin films prepared by laser ablation. Journal of Applied Physics, 2004, 95, 241-247.	2.5	73
38	The influence of preparation conditions on electrochemical properties of LiNi0.5Mn1.5O4 thin film electrodes by PLD. Electrochimica Acta, 2007, 52, 2822-2828.	5.2	72
39	Texture effect on the electrochemical properties of LiCoO2 thin films prepared by PLD. Electrochimica Acta, 2007, 52, 7014-7021.	5.2	71
40	Influence of crystallization temperature on ionic conductivity ofÂlithium aluminum germanium phosphate glass-ceramic. Journal of Power Sources, 2015, 290, 123-129.	7.8	71
41	Monodisperse Li1.2Mn0.6Ni0.2O2 microspheres with enhanced lithium storage capability. Journal of Materials Chemistry A, 2013, 1, 5301.	10.3	66
42	Study on Shrinkage Behaviour of Direct Laser Sintering Metallic Powder. Proceedings of the Institution of Mechanical Engineers, Part B: Journal of Engineering Manufacture, 2006, 220, 183-190.	2.4	65
43	Achieving high energy density in a 4.5 V all nitrogen-doped graphene based lithium-ion capacitor. Journal of Materials Chemistry A, 2019, 7, 19909-19921.	10.3	65
44	Hierarchical Porous Intercalationâ€Type V <sub>2</sub> O <sub>3</sub> as Highâ€Performance Anode Materials for Liâ€Ion Batteries. Chemistry - A European Journal, 2017, 23, 7538-7544.	3.3	63
45	Deactivation of a Single-Site Gold-on-Carbon Acetylene Hydrochlorination Catalyst: An X-ray Absorption and Inelastic Neutron Scattering Study. ACS Catalysis, 2018, 8, 8493-8505.	11.2	63
46	Inorganic sodium solid-state electrolyte and interface with sodium metal for room-temperature metal solid-state batteries. Energy Storage Materials, 2021, 34, 28-44.	18.0	63
47	Photocrosslinkable nanocomposite ink for printing strong, biodegradable and bioactive bone graft. Biomaterials, 2020, 263, 120378.	11.4	61
48	High electric breakdown strength and energy density in vinylidene fluoride oligomer/poly(vinylidene) Tj ETQq0 0	0 rggT /Ov	erlock 10 Tf
49	Revealing Mechanism of Li <sub>3</sub> PO <sub>4</sub> Coating Suppressed Surface Oxygen Release for Commercial Ni-Rich Layered Cathodes. ACS Applied Energy Materials, 2020, 3, 7445-7455.	5.1	58
50	Temperature-Dependent Lithium-Ion Diffusion and Activation Energy of Li <sub>1.2</sub> Co <sub>0.13</sub> Ni <sub>0.13</sub> Mn <sub>0.54</sub> O <sub>2</sub> Thin-Film Cathode at Nanoscale by Using Electrochemical Strain Microscopy. ACS Applied Materials & Interfaces, 2017, 9, 13999-14005.	8.0	55
51	Thermal and compositional driven relaxor ferroelectric behaviours of lead-free Bi <sub>0.5</sub> Na <sub>0.5</sub> TiO <sub>3</sub> –SrTiO <sub>3</sub> ceramics. Journal of Materials Chemistry C, 2020, 8, 2411-2418.	5.5	54
52	Study on vacancy formation in ferroelectric PbTiO3 from ab initio. Applied Physics Letters, 2006, 88, 142902.	3.3	53
53	Ultrathin Nanoribbons of in Situ Carbon-Coated V <sub>3</sub> O <sub>7</sub> ·H <sub>2</sub> O for High-Energy and Long-Life Li-Ion Batteries: Synthesis, Electrochemical Performance, and Chargeâ€"Discharge Behavior. ACS Applied Materials & Interfaces, 2017, 9, 17002-17012.	8.0	53

54Transport and electrochemical properties of high potential tavorite LiVPO4F. Solid State Ionics, 2013,<br/>242, 10-19.2.752

#	Article	IF	CITATIONS
55	Manganese oxide thin films prepared by pulsed laser deposition for thin film microbatteries. Materials Chemistry and Physics, 2014, 143, 720-727.	4.0	50
56	Crystal structure, migration mechanism and electrochemical performance of Cr-stabilized garnet. Solid State Ionics, 2014, 268, 135-139.	2.7	50
57	Recent advances of bismuth based anode materials for sodium-ion batteries. Materials Technology, 2018, 33, 563-573.	3.0	50
58	Microstructural and Electrochemical Properties of Al- and Ga-Doped Li <sub>7</sub> La <sub>3</sub> Zr <sub>2</sub> O <sub>12</sub> Garnet Solid Electrolytes. ACS Applied Energy Materials, 2020, 3, 4708-4719.	5.1	50
59	Intermolecular interactions and high dielectric energy storage density in poly(vinylidene) Tj ETQq1 1 0.784314 rg	gBT /Overlo 3.3	ock 10 Tf 50 3 49
60	Three-dimensional hierarchical nickel–cobalt–sulfide nanostructures for high performance electrochemical energy storage electrodes. Journal of Materials Chemistry A, 2016, 4, 18335-18341.	10.3	49
61	Role of carbon coating in improving electrochemical performance of Li-rich Li(Li <sub>0.2</sub> Mn <sub>0.54</sub> Ni <sub>0.13</sub> Co <sub>0.13</sub> )O <sub>2</sub> cathode. RSC Advances, 2014, 4, 44244-44252.	3.6	48
62	Substantial doping engineering in Na3V2-xFex(PO4)3 (0â‰ <b>¤</b> â‰ <b>0</b> .15) as high-rate cathode for sodium-ion battery. Materials and Design, 2020, 186, 108287.	7.0	48
63	Structure and properties of hot-pressed lead-free (Ba0.85Ca0.15)(Zr0.1Ti0.9)O3 piezoelectric ceramics. RSC Advances, 2013, 3, 20693.	3.6	47
64	1.8 V symmetric supercapacitors developed using nanocrystalline Ru films as electrodes. RSC Advances, 2014, 4, 11111.	3.6	47
65	Cycling effects on surface morphology, nanomechanical and interfacial reliability of LiMn2O4 cathode in thin film lithium ion batteries. Electrochimica Acta, 2012, 68, 52-59.	5.2	44
66	Chemical Bonding Construction of Reduced Graphene Oxide-Anchored Few-Layer Bismuth Oxychloride for Synergistically Improving Sodium-Ion Storage. Chemistry of Materials, 2019, 31, 7311-7319.	6.7	44
67	Elevating the discharge plateau of prussian blue analogs through low-spin Fe redox induced intercalation pseudocapacitance. Energy Storage Materials, 2021, 43, 182-189.	18.0	43
68	NASICON-Structured LiGe <sub>2</sub> (PO <sub>4</sub> ) <sub>3</sub> with Improved Cyclability for High-Performance Lithium Batteries. Journal of Physical Chemistry C, 2009, 113, 20514-20520.	3.1	42
69	Probing the Coexistence of Ferroelectric and Relaxor States in Bi <sub>0.5</sub> Na <sub>0.5</sub> TiO <sub>3</sub> Based Ceramics for Enhanced Piezoelectric Performance. ACS Applied Materials & Interfaces, 2020, 12, 30548-30556.	8.0	41
70	Mesoporous Li <sub>4</sub> Ti <sub>5</sub> O <sub>12â^'x</sub> /C submicrospheres with comprehensively improved electrochemical performances for high-power lithium-ion batteries. Physical Chemistry Chemical Physics, 2014, 16, 24874-24883.	2.8	40
71	Grain boundary effects on Li-ion diffusion in a Li <sub>1.2</sub> Co <sub>0.13</sub> Ni <sub>0.13</sub> Mn <sub>0.54</sub> O <sub>2</sub> thin film cathode studied by scanning probe microscopy techniques. RSC Advances, 2016, 6, 94000-94009.	3.6	40
72	Extra Sodiation Sites in Hard Carbon for High Performance Sodium Ion Batteries. Small Methods, 2021, 5, e2100580.	8.6	40

#	Article	IF	CITATIONS
73	Pulsed laser deposition of lead-zirconate-titanate thin films and multilayered heterostructures. Applied Physics A: Materials Science and Processing, 2005, 81, 701-714.	2.3	39
74	Synthesis and properties of poly(1,3-dioxolane) <i>in situ</i> quasi-solid-state electrolytes <i>via</i> a rare-earth triflate catalyst. Chemical Communications, 2021, 57, 7934-7937.	4.1	39
75	A Robust Solid–Solid Interface Using Sodium–Tin Alloy Modified Metallic Sodium Anode Paving Way for Allâ€ <del>S</del> olidâ€State Battery. Advanced Energy Materials, 2021, 11, 2101228.	19.5	39
76	Nanoscale characterization of charged/discharged lithium-rich thin film cathode by scanning probe microscopy techniques. Journal of Power Sources, 2017, 352, 9-17.	7.8	38
77	Effect of bottom electrodes on nanoscale switching characteristics and piezoelectric response in polycrystalline BiFeO3 thin films. Journal of Applied Physics, 2011, 110, .	2.5	37
78	In-situ nanoscale mapping of surface potential in all-solid-state thin film Li-ion battery using Kelvin probe force microscopy. Journal of Applied Physics, 2012, 111, .	2.5	37
79	Improvement of Li ion conductivity of Li 5 La 3 Ta 2 O 12 solid electrolyte by substitution of Ge for Ta. Journal of Power Sources, 2017, 349, 105-110.	7.8	37
80	IMPROVED CAPACITIVE BEHAVIOR OF <font>MnO</font> <sub>2</sub> THIN FILMS PREPARED BY ELECTRODEPOSITION ON THE PT SUBSTRATE WITH A <font>MnO</font> <sub>x</sub> BUFFER LAYER. Functional Materials Letters, 2009, 02, 13-18.	1.2	36
81	One-pot high temperature hydrothermal synthesis of Fe3O4@C/graphene nanocomposite as anode for high rate lithium ion battery. Electrochimica Acta, 2015, 180, 1041-1049.	5.2	36
82	Growth of layered LiNi0.5Mn0.5O2 thin films by pulsed laser deposition for application in microbatteries. Applied Physics Letters, 2008, 92, .	3.3	35
83	Properties of nano-crystalline LiMn2O4 thin films deposited by pulsed laser deposition. Electrochimica Acta, 2006, 52, 1161-1168.	5.2	34
84	Flexible, stable, fast-ion-conducting composite electrolyte composed of nanostructured Na-super-ion-conductor framework and continuous Poly(ethylene oxide) for all-solid-state Na battery. Journal of Power Sources, 2020, 454, 227949.	7.8	34
85	Insight into the structure-capacity relationship in biomass derived carbon for high-performance sodium-ion batteries. Journal of Energy Chemistry, 2021, 62, 497-504.	12.9	34
86	Mitigated phase transition during first cycle of a Li-rich layered cathode studied by in operando synchrotron X-ray powder diffraction. Physical Chemistry Chemical Physics, 2016, 18, 4745-4752.	2.8	33
87	Preparation of Nanocomposite Polymer Electrolyte via In Situ Synthesis of SiO2 Nanoparticles in PEO. Nanomaterials, 2020, 10, 157.	4.1	32
88	Poly(vinylidene fluoride-co-hexafluoropropylene)-graft-poly(dopamine methacrylamide) copolymers: A nonlinear dielectric material for high energy density storage. Applied Physics Letters, 2013, 103, .	3.3	31
89	Research Update: Ca doping effect on the Li-ion conductivity in NASICON-type solid electrolyte LiZr2(PO4)3: A first-principles molecular dynamics study. APL Materials, 2018, 6, .	5.1	31
90	Allâ€Solidâ€State Thin Film μâ€Batteries for Microelectronics. Advanced Science, 2021, 8, e2100774.	11.2	31

#	Article	IF	CITATIONS
91	Formation of Magnesium Silicide by Mechanical Alloying. Materials Technology, 1997, 4, 275-283.	0.3	30
92	Comparative study of LiMn2O4 thin film cathode grown at high, medium and low temperatures by pulsed laser deposition. Journal of Solid State Chemistry, 2006, 179, 3831-3838.	2.9	30
93	<font>Li</font> -rich layer-structured cathode materials for high energy <font>Li</font> -ion batteries. Functional Materials Letters, 2014, 07, 1430002.	1.2	30
94	Operando X-ray Absorption Spectroscopy Study of Atomic Phase Reversibility with Wavelet Transform in the Lithium-Rich Manganese Based Oxide Cathode. Chemistry of Materials, 2016, 28, 4191-4203.	6.7	30
95	Composite Hybrid Quasi-Solid Electrolyte for High-Energy Lithium Metal Batteries. ACS Applied Energy Materials, 2021, 4, 7973-7982.	5.1	30
96	Li1.5Al0.5Ge1.5(PO4)3 Li-ion conductor prepared by melt-quench and low temperature pressing. Solid State lonics, 2015, 278, 65-68.	2.7	29
97	Grain growth and recrystallization of nanocrystalline Al3Ti prepared by mechanical alloying. Journal of Materials Science, 2003, 38, 613-619.	3.7	28
98	A facile strategy to achieve high conduction and excellent chemical stability of lithium solid electrolytes. RSC Advances, 2015, 5, 6588-6594.	3.6	28
99	Intrinsic low sodium/NASICON interfacial resistance paving the way for room temperature sodium-metal battery. Journal of Colloid and Interface Science, 2021, 601, 418-426.	9.4	28
100	Local probing of magnetoelectric coupling and magnetoelastic control of switching in BiFeO3-CoFe2O4 thin-film nanocomposite. Applied Physics Letters, 2013, 103, 042906.	3.3	27
101	Selective Laser Sintering of Porous Silica Enabled by Carbon Additive. Materials, 2017, 10, 1313.	2.9	26
102	A facile method for the synthesis of a sintering dense nano-grained Na <sub>3</sub> Zr <sub>2</sub> Si <sub>2</sub> PO <sub>12</sub> Na <sup>+</sup> -ion solid-state electrolyte. Chemical Communications, 2021, 57, 4023-4026.	4.1	26
103	Ultrathin carbon nanopainting of LiFePO4 by oxidative surface polymerization of dopamine. Journal of Power Sources, 2014, 265, 239-245.	7.8	25
104	Na-rich layered Na2Ti1â~'xCrxO3â~'x/2 (x = 0, 0.06): Na-ion battery cathode materials with high capacity long cycle life. Scientific Reports, 2017, 7, 373.	and 3.3	25
105	Preparation of thin solid electrolyte by hot-pressing and diamond wire slicing. RSC Advances, 2019, 9, 11670-11675.	3.6	25
106	Facile aqueous synthesis of high performance Na <sub>2</sub> FeM(SO <sub>4</sub> ) <sub>3</sub> (M =) Tj ETC 2728-2740.	2q0 0 0 rg 10.3	BT /Overloc 25
107	Li diffusion in spinel LiNi <sub>0.5</sub> Mn <sub>1.5</sub> O <sub>4</sub> thin films prepared by pulsed laser deposition. Physica Scripta, 2007, T129, 43-48.	2.5	24

<sup>108</sup>Li diffusion in LiNi0.5Mn0.5O2 thin film electrodes prepared by pulsed laser deposition. Electrochimica<br/>Acta, 2009, 54, 5986-5991.5.224

#	Article	IF	CITATIONS
109	Roles of Alkaline Earth Ions in Garnetâ€Type Superionic Conductors. ChemElectroChem, 2017, 4, 266-271.	3.4	23
110	A new approach for synthesizing bulk-type all-solid-state lithium-ion batteries. Journal of Materials Chemistry A, 2019, 7, 9748-9760.	10.3	23
111	Dual-Nitrogen-Doped Carbon Decorated on Na <sub>3</sub> V <sub>2</sub> (PO <sub>4</sub> ) <sub>3</sub> to Stabilize the Intercalation of Three Sodium Ions. ACS Applied Energy Materials, 2020, 3, 6870-6879.	5.1	23
112	Understanding and Preventing Dendrite Growth in Lithium Metal Batteries. ACS Applied Materials & Interfaces, 2021, 13, 34320-34331.	8.0	23
113	ELECTROCHEMICAL PROPERTIES OF BIFeO3 THIN FILMS PREPARED BY PULSED LASER DEPOSITION. Functional Materials Letters, 2009, 02, 163-167.	1.2	22
114	Leakage behavior and conduction mechanisms of Ba(Ti0.85Sn0.15)O3/Bi1.5Zn1.0Nb1.5O7 heterostructures. Journal of Applied Physics, 2010, 107, .	2.5	22
115	Li5Cr9Ti4O24: A new anode material for lithium-ion batteries. Journal of Alloys and Compounds, 2015, 650, 616-621.	5.5	22
116	Ferroelectric Engineered Electrodeâ€Composite Polymer Electrolyte Interfaces for Allâ€Solidâ€State Sodium Metal Battery. Advanced Science, 2022, 9, e2105849.	11.2	22
117	Synthesis mechanism of an Al-Ti-C grain refiner master alloy prepared by a new method. Metallurgical and Materials Transactions A: Physical Metallurgy and Materials Science, 2003, 34, 1727-1733.	2.2	21
118	Abnormal grain growth of WC with small amount of cobalt. Philosophical Magazine, 2007, 87, 5657-5671.	1.6	21
119	Electronic Coupling of Cobalt Nanoparticles to Nitrogenâ€Đoped Graphene for Oxygen Reduction and Evolution Reactions. ChemSusChem, 2016, 9, 3067-3073.	6.8	21
120	Alleviating mechanical degradation of hexacyanoferrate via strain locking during Na+ insertion/extraction for full sodium ion battery. Nano Research, 2022, 15, 2123-2129.	10.4	21
121	Magnetic and Microstructural Properties of CoCrPt:Oxide Perpendicular Recording Media With Novel Intermediate Layers. IEEE Transactions on Magnetics, 2007, 43, 633-638.	2.1	20
122	Structural and Electrochemical Properties of LiNi[sub 0.5]Mn[sub 0.5]O[sub 2] Thin-Film Electrodes Prepared by Pulsed Laser Deposition. Journal of the Electrochemical Society, 2010, 157, A348.	2.9	20
123	In operando X-ray absorption spectroscopy study of charge rate effects on the atomic environment in graphene-coated Li-rich mixed oxide cathode. Materials and Design, 2016, 98, 231-242.	7.0	20
124	Synergistic Effect for LiMn2O4Microcubes with Enhanced Rate Capability and Excellent Cycle Stability for Lithium Ion Batteries. Journal of the Electrochemical Society, 2016, 163, A197-A202.	2.9	20
125	Gallium-substituted Nasicon Na3Zr2Si2PO12 solid electrolytes. Journal of Alloys and Compounds, 2021, 855, 157501.	5.5	20
126	Defect and electronic structures of acceptor substituted lead titanate. Applied Physics Letters, 2008, 92, 112909.	3.3	19

#	Article	IF	CITATIONS
127	Influence of oxygen pressure on the ferroelectric properties ofÂBiFeO3 thin films on LaNiO3/Si substrates via laser ablation. Applied Physics A: Materials Science and Processing, 2010, 101, 651-654.	2.3	19
128	Deformation behaviour of ultrafine and nanosize-grained Mg alloy synthesized via mechanical alloying. Philosophical Magazine, 2006, 86, 2919-2939.	1.6	18
129	The role of oxygen pressure and thickness on structure and pyroelectric properties of Ba(Ti0.85Sn0.15)O3 thin films grown by pulsed laser deposition. Journal of Applied Physics, 2009, 105, 084102.	2.5	18
130	Cycling Effect on Morphological and Interfacial Properties of RuO2 Anode Film in Thin-Film Lithium Ion Microbatteries. Metallurgical and Materials Transactions A: Physical Metallurgy and Materials Science, 2013, 44, 26-34.	2.2	18
131	Study on stabilization of cubic Li <sub>7</sub> La <sub>3</sub> Zr <sub>2</sub> O12 by Ge substitution in various atmospheres. Functional Materials Letters, 2016, 09, 1642005.	1.2	18
132	3D Frameworks with Variable Magnetic and Electrical Features from Sintered Cobalt-Modified Carbon Nanotubes. ACS Applied Materials & Interfaces, 2018, 10, 20983-20994.	8.0	18
133	Multi-substituted garnet-type electrolytes for solid-state lithium batteries. Ceramics International, 2020, 46, 5489-5494.	4.8	18
134	The manufacture of micromould and microparts by vacuum casting. International Journal of Advanced Manufacturing Technology, 2008, 38, 944-948.	3.0	17
135	Role of Pb(Zr0.52Ti0.48)O3 substitution in multiferroic properties of polycrystalline BiFeO3 thin films. Journal of Applied Physics, 2011, 110, .	2.5	17
136	ELECTROCHEMICAL PROPERTY OF <font>LiMn<sub>2</sub>O<sub>4</sub></font> IN OVER-DISCHARGED CONDITIONS. Functional Materials Letters, 2012, 05, 1250028.	1.2	17
137	Processing and characterization of laser-sintered Al2O3/ZrO2/SiO2. International Journal of Advanced Manufacturing Technology, 2013, 68, 2565-2569.	3.0	17
138	Micro-rapid-prototyping via multi-layered photo-lithography. International Journal of Advanced Manufacturing Technology, 2006, 29, 1026-1032.	3.0	15
139	Decomposition failure of Li1.5Al0.5Ge1.5(PO4)3 solid electrolytes induced by electric field: A multi-scenario study using Scanning Probe Microscopy-based techniques. Journal of Power Sources, 2020, 471, 228468.	7.8	15
140	Fractal-based description for the three-dimensional surface of materials. Journal of Applied Physics, 1999, 86, 2526-2532.	2.5	14
141	Electromechanical Failure of NASICON-Type Solid-State Electrolyte-Based All-Solid-State Li-Ion Batteries. Chemistry of Materials, 2021, 33, 6841-6852.	6.7	14
142	Controllable 3D Porous Ni Current Collector Coupled with Surface Phosphorization Enhances Na Storage of Ni <sub>3</sub> S <sub>2</sub> Nanosheet Arrays. Small, 2022, 18, e2106161.	10.0	14
143	Enhanced tunable and pyroelectric properties of Ba(Ti0.85Sn0.15)O3 thin films with Bi1.5Zn1.0Nb1.5O7 buffer layers. Applied Physics Letters, 2010, 96, .	3.3	13
144	Thickness dependence of structure, tunable and pyroelectric properties of laser-ablated Ba(Zr <sub>0.25</sub> Ti <sub>0.75</sub> )O <sub>3</sub> thin films. Journal Physics D: Applied Physics, 2010, 43, 035402.	2.8	13

#	Article	IF	CITATIONS
145	Orientation-dependent surface potential behavior in Nb-doped BiFeO3. Applied Physics Letters, 2012, 100, .	3.3	13
146	Fe3O4/rice husk-based maco-/mesoporous carbon bone nanocomposite as superior high-rate anode for lithium ion battery. Journal of Solid State Electrochemistry, 2017, 21, 27-34.	2.5	13
147	Dual Substitution and Spark Plasma Sintering to Improve Ionic Conductivity of Garnet Li7La3Zr2O12. Nanomaterials, 2019, 9, 721.	4.1	13
148	Rice Huskâ€Based 3D Porous Silicon/Carbon Nanocomposites as Anode for Lithiumâ€lon Batteries. Energy Technology, 2019, 7, 1800787.	3.8	13
149	Abnormal Ionic Conductivities in Halide NaBi <sub>3</sub> O <sub>4</sub> Cl <sub>2</sub> Induced by Absorbing Water and a Derived Oxhydryl Group. Angewandte Chemie - International Edition, 2020, 59, 8991-8997.	13.8	13
150	The role of amorphous Ni50P50 precoating layer in CoCrPtTa thin film media. Journal of Applied Physics, 2000, 87, 6346-6348.	2.5	12
151	The mechanical alloying of titanium aluminides. Jom, 2002, 54, 62-64.	1.9	12
152	Vortex structure transformation of BaTiO3 nanoparticles through the gradient function. Journal of Applied Physics, 2009, 106, .	2.5	12
153	Cycling effects on interfacial reliability of TiO2 anode film in thin film lithium-ion microbatteries. Journal of Solid State Electrochemistry, 2012, 16, 1877-1881.	2.5	12
154	Increasing the high rate performance of mixed metal phospho-olivine cathodes through collective and cooperative strategies. Journal of Power Sources, 2014, 247, 273-279.	7.8	12
155	Magnetic, ferroelectric, and dielectric properties of Bi(Sc0.5Fe0.5)O3–PbTiO3 thin films. Journal of Applied Physics, 2009, 105, 074101.	2.5	11
156	Hollow microspherical LiFePO4/C synthesized from a novel multidentate phosphonate complexing agent. RSC Advances, 2013, 3, 5127.	3.6	11
157	Dual arbon Network for the Effective Transport of Charged Species in a LiFePO <sub>4</sub> Cathode for Lithiumâ€lon Batteries. Energy Technology, 2015, 3, 63-69.	3.8	11
158	Fe–P–S electrodes for all-solid-state lithium secondary batteries using sulfide-based solid electrolytes. Journal of Power Sources, 2020, 449, 227576.	7.8	11
159	Stabilization of cubic Li7La3Zr2O12 by Al substitution in various atmospheres. Solid State Ionics, 2020, 350, 115323.	2.7	11
160	Solid-gas reactions driven by mechanical alloying of niobium and tantalum in nitrogen. Metallurgical and Materials Transactions A: Physical Metallurgy and Materials Science, 1999, 30, 1097-1100.	2.2	10
161	Phase diagram of NaFeyCo1-yO2 and evolution of its physico- and electrochemical properties with changing iron content. Journal of Power Sources, 2019, 419, 42-51.	7.8	10
162	Li3.33Cu1.005Ti4.665O12/CuO composite with P4332 space group for Li-ion batteries: synergistic effect of substituting and compositing. RSC Advances, 2014, 4, 31196-31200.	3.6	9

#	Article	IF	CITATIONS
163	Abnormal Phenomena of Multiâ€Way Sodium Storage in Selenide Electrode. Advanced Functional Materials, 2021, 31, 2102406.	14.9	9
164	The effect of O3–P3–Pâ€23 phases coexistence in NaxFe0.3Co0.7O2 cathode material on its electronic and electrochemical properties. Experimental and theoretical studies. Journal of Power Sources, 2020, 449, 227471.	7.8	8
165	Laser induced transformation of TiSi2. Journal of Applied Physics, 2003, 94, 4291-4295.	2.5	7
166	Characterization of crystallized LiMn <sub>2</sub> O <sub>4</sub> thin films grown by pulsed laser deposition. Philosophical Magazine, 2007, 87, 3249-3258.	1.6	7
167	Doping Induced Hierarchical Lattice Expansion of Cobalt Diselenide/Carbon Nanosheet Hybrid for Fast and Stable Sodium Storage. Cell Reports Physical Science, 2020, 1, 100082.	5.6	7
168	Reactive Synthesis of NbAl3 Matrix Composites. Materials Research Society Symposia Proceedings, 1990, 194, 79.	0.1	6
169	Trap State Spectroscopy of LiM <sub><i>y</i></sub> Mn <sub>2-y</sub> O <sub>4</sub> (M = Mn, Ni, Co): Guiding Principles for Electrochemical Performance. Journal of Physical Chemistry C, 2013, 117, 3812-3817.	3.1	6
170	Hierarchical porous CoO /carbon nanocomposite for enhanced lithium storage. Journal of Electroanalytical Chemistry, 2019, 847, 113202.	3.8	6
171	Ammonium escorted chloride chemistry in stabilizing aqueous chloride ion battery. Materials Today Energy, 2022, 26, 101020.	4.7	6
172	Effect of Matrix Constitution on Microstructure and Mechanical Properties of Rheocast Metal Matrix Composites. Materials and Manufacturing Processes, 1998, 13, 27-52.	4.7	5
173	Title is missing!. Journal of Materials Science, 1999, 34, 1681-1689.	3.7	5
174	Highly (100) oriented Pb(Zr0.52Ti0.48)O3/LaNiO3 films grown on amorphous substrates by pulsed laser deposition. Applied Physics A: Materials Science and Processing, 2007, 88, 365-370.	2.3	5
175	Development of a drop-on-demand system for multiple material dispensing. , 2008, , .		5
176	ELECTRIC, MAGNETIC AND MECHANICAL COUPLING EFFECTS ON FERROELECTRIC PROPERTIES AND SURFACE POTENTIAL OF <font>BiFeO</font> <sub>3</sub> THIN FILM. Functional Materials Letters, 2011, 04, 91-95.	1.2	5
177	Nanocomposite multilayer capacitors comprising <font>BaTiO</font> <sub>3</sub> @ <font>TiO</font> <sub>2</sub> and poly(vinylidene) Tj ETQq1 1 0.784314 r 2014. 04. 1450009.	gBT /Over 2.4	lgck 10 Tf 5(
178	Ultrathin, Compacted Gel Polymer Electrolytes Enable Highâ€Energy and Stableâ€Cycling 4â€V Lithiumâ€Metal Batteries. ChemElectroChem, 2020, 7, 3656-3662.	3.4	5
179	STEP-FLOW GROWTH OF HETEROEPITAXIAL <font>SrRuO</font> <sub>3</sub> THIN FILMS ON 0.04° <font>SrTiO</font> <sub>3</sub> (001) VICINAL SUBSTRATES. Functional Materials Letters, 2008, 01, 253-257.	1.2	4
180	Strain effect on the surface potential and nanoscale switching characteristics of multiferroic BiFeO3 thin films. Applied Physics Letters, 2012, 100, 132907.	3.3	4

#	Article	IF	CITATIONS
181	Ultrathin, dense, hybrid polymer/ceramic gel electrolyte for high energy lithium metal batteries. Materials Letters, 2020, 279, 128480.	2.6	4
182	Scalable Li <sub>1.5</sub> Al <sub>0.5</sub> Ge <sub>1.5</sub> (PO <sub>4</sub> ) <sub>3</sub> thin membrane prepared by tape-casting for large-scale lithium–air battery application. Materials Technology, 2020, 35, 572-579.	3.0	4
183	Structural, thermal, and electrochemical studies of biodegradable gel polymer electrolyte for electric double layer capacitor. High Performance Polymers, 2022, 34, 673-682.	1.8	4
184	Formation of Micromoulds via UV Lithography of SU8 Photoresist and Nickel Electrodeposition. Proceedings of the Institution of Mechanical Engineers, Part B: Journal of Engineering Manufacture, 2006, 220, 329-333.	2.4	3
185	Highâ€Power and Highâ€Energy Cuâ€Substituted Li x Ni 0.88– y Co y Mn 0.1 Cu 0.02 O 2 Cathode Material for Liâ€Ion Batteries. Physica Status Solidi (A) Applications and Materials Science, 2020, 217, 1900951.	1.8	3
186	Supercapacitors Based on Activated Carbons, Products of Rice Hull Processing. Russian Journal of Physical Chemistry A, 2021, 95, 818-826.	0.6	3
187	Response and Implication of NASICON Solid-State Electrolytes to Local Electrical Stimulation: From Surface Engineering to Interfacial Manipulation. ACS Applied Materials & Interfaces, 2021, 13, 46588-46597.	8.0	3
188	Mechanochemical Activation of Solid State Reaction between Mg and TiO2. JSME International Journal Series A-Solid Mechanics and Material Engineering, 2003, 46, 251-254.	0.4	2
189	ACCEPTOR MODULATED DEFECT AND ELECTRONIC STRUCTURES IN FERROELECTRIC LEAD TITANATE: AN AB INITIO STUDY. Functional Materials Letters, 2008, 01, 121-126.	1.2	2
190	Low temperature sintering of crystallized Li1.5Al0.5Ge1.5(PO4)3 using hot-press technique. Materials Today: Proceedings, 2019, 17, 408-415.	1.8	2
191	Fast discharge–charge properties of FePS3 electrode for all-solid-state batteries using sulfide electrolytes and its stable diffusion path. Functional Materials Letters, 2021, 14, 2141005.	1.2	2
192	Porous Li2O Al2O3SiO2(LAS) Glass-Ceramics Prepared by Selective Laser Melting and Annealing. Ceramic Engineering and Science Proceedings, 0, , 523-528.	0.1	2
193	Excimer laser-induced transformation in laser ablated Pb(Zr0.52Ti0.48)O3amorphous thin films. Philosophical Magazine, 2004, 84, 3729-3739.	1.6	1
194	ELECTROCHEMICAL PERFORMANCE OF MICROBATTERIES USING CRYSTALLIZED <font>LiCoO</font> <sub>2</sub> AND NANO-CRYSTALLINE <font>LiMn</font> <sub>2</sub> <font>O</font> <sub>4</sub> FILM AS CATHODES AND AMORPHOUS <font>LiNiVO</font> <sub>4</sub> AS ANODE. Surface Review and Letters, 2008, 15, 169-174.	1.1	1
195	THE BEHAVIOR OF ELECTRODEPOSITED NANOCRYSTALLINE <font>Co–Ni</font> ALLOYS SUBJECTED TO MAGNETIC AND STRESS FIELDS. Surface Review and Letters, 2010, 17, 129-134.	1.1	1
196	Abnormal Ionic Conductivities in Halide NaBi 3 O 4 Cl 2 Induced by Absorbing Water and a Derived Oxhydryl Group. Angewandte Chemie, 2020, 132, 9076-9082.	2.0	1
197	Effect of silicon substrate amorphization on the kinetics of reaction between a titanium thin film and silicon. Philosophical Magazine A: Physics of Condensed Matter, Structure, Defects and Mechanical Properties, 2002, 82, 2923-2934.	0.6	0
198	Kinetics of ß-phase transformation in the heat treatment of FeSi2- and Fe2Si5-based thermoelectric alloys. Philosophical Magazine, 2003, 83, 2865-2873.	1.6	0

#	Article	IF	CITATIONS
199	Novel Approach to Reduce Grain Size in CoCrPt-Oxide Perpendicular Recording Media. , 2006, , .		0
200	Deformation behaviour of nanocrystalline Mg-Al alloys during nanoindentation. , 2010, , .		0
201	COMPRESSIVE BEHAVIOUR OF NANOCRYSTALLILNE Mg-5%Al ALLOYS. , 2011, , .		Ο
202	Interface between Sodium Metal and Nasicon Solid-State Electrolyte. ECS Meeting Abstracts, 2020, MA2020-02, 833-833.	0.0	0
203	Growth of Lanio3 Films by Pulsed Laser Deposition. Ceramic Engineering and Science Proceedings, 0, , 51-55.	0.1	0
204	Thin Nasicon Sodium-Ions Solid State Electrolyte By Tape Casting Method. ECS Meeting Abstracts, 2022, MA2022-01, 499-499.	0.0	0